ISSN: 0974-5823 Vol. 7 No. 10 October, 2022

International Journal of Mechanical Engineering

Tunable Optical Bandgap of $La_{0.7}Sr_{0.15}Ca_{0.15}MnO_3$ Nanocrystallites: Impact of Annealing Temperature on Optical properties

Mohd Abdul Shukur[1,2], K. Vijaya Kumar[1*], G. Narsinga Rao[3]

[1]Department of Physics, JNTUH University College of Engineering Rajanna Sircilla, Agraharam, Rajanna Sircilla-District, 505302, TS, India.

[2]Department of Physics, SRR Government Arts & Science College (Autonomous), Karimnagar, 505001, Telangana, India.

[3]Department of Physics, Marri Laxman Reddy Institute of Technology and Management, Dundigal, Hyderabad 500043, Telangana, India.

Abstract

Nanocrystalline $La_{0.7}Sr_{0.15}Ca_{0.15}MnO_3$ manganite was synthesised using the Solgel-combustion method and annealed at various temperatures (T_A). XRD patterns confirmed the formation of a Rhombohedral structure $R\bar{3}c$.There was a growth in crystallite size from 15.6 to 36.8 nm as T_A increased from 700 to 1300°C. The dislocation density and microstrain were decreased as a function of annealed temperatures. The characteristic absorbance peaks were found around 447nm in the Visible range. The refractive index, reflectance, extinction coefficient, and real, imaginary part of dielectric constant of all samples were varied as function of annealed temperature. The optical energy gaps of $La_{0.7}Sr_{0.15}Ca_{0.15}MnO_3$ nanocrystalline were found to decrease from 3.59 to 3.41 eV with the rise in temperature. Hence, $La_{0.7}Sr_{0.15}Ca_{0.15}MnO_3$ nanocrystallites show novel optical properties as a function of calcination temperatures.

Keywords: *XRD, Band gap, Refractive index.*

*Corresponding author kvkphd@gmail.com (Katrapally Vijaya Kumar)

1.Introduction

Magneto resistance materials are an important topic in science and research because they have more advantages than typical magnetic materials in terms of structural, physical, and magnetic properties. Storage technologies, biomedical applications and micro electrical devices are only a few of the applications for these materials. These materials are utilized to create cooling systems that have a high cooling efficiency while producing minimal noise, emit no greenhouse gases and are environmentally beneficial [1,2].Lanthanum doped perovskite type manganite oxides substituted by divalent alkaline earth ions exhibits interesting properties like colossal magnetoresistance (CMR), metal to insulating behaviour (MI transition)[3-7].Doping with a divalent ion into La sites, Mn^{3+} ions are transformed into Mn^4 ions, resulting

into double exchange between $Mn^{3+}$and Mn^{4+} with electronic configuration, ($3d^4$, $t^3_{2g}\uparrow e^1_g\uparrow$, S=2) and ($3d^3$,$t^3_{2g}\uparrow e^0_g\uparrow$, S=3/2),which mediates the ferromagnetic interaction. Mn-O bond length and Mn-O-Mn bond angles, which are controlled by A and B sites ionic radii and Mn^{3+}/ Mn^{4+} ratio and alters the double exchange interaction. These effects the strongly on magneto resistive properties of the perovskite manganite [8]. These materials also exhibit a high Seebeck coefficient (also known as thermos electrical power). The characteristic behaviour of these manganite drastically changes due to the concentration of substitution at La site [9-14]. Lanthanum doped perovskite type manganite are fascinating and demanding materials because of these characteristics. With the rapid integration and downsizing of electronic devices, these perovskite manganites are prepared in nanoscale. The relationship among structural, orbital, and electronic degrees of freedom can be explored further to fully comprehend the complicated science behind rare – earth manganite features.

Manganite's transport and magnetic properties are affected by their crystalline size [15,16]. The sintering temperature can affect grain size, therefore increasing the sintering temperature should increase grain growth [17,18]. Due to its intriguing properties, like huge ratio between surface to volume and surface effect, research on perovskite manganite with nanoscale particle sies has grown in recent years. The high bandwidth of the MI transition in $La_{1-x}Sr_xMnO_3$ and the small band width of MI transition and colossal magneto resistance effect in $La_{1-x}Ca_xMnO_3$ were described by process of the double exchange (DE) interaction [19,20,22].

Different physical and optical properties are obtained by combining $La_{1-x}Sr_xMnO_3$ with $La_{1-x}Ca_xMnO_3$ in the appropriate ratio. Calcium doped Strontium – Lanthanum manganite exhibit remarkable properties as a high magnetocaloric material among divalent ions [21]. The nanoscale manganites have novel characteristics which varies with particle size when compared to those bulk materials. Because manganite nanoparticles are primarily metal conductors, only a few prior research has been done on their optical characteristics. Among several investigations using $La_{1-x}Sr_xMnO_3$ and $La_{1-x}Ca_xMnO_3$, only a handful had revealed coexisting Ca and Sr systems. The Solgel-combustion preparation method was used in this research to synthesise $La_{0.7}Sr_{0.15}Ca_{0.15}MnO_3$ nanocrystallites because of its convenience of use, low cost, and modest sintering temperature for nanocrystallites. This method also enables the production of $La_{0.7}Sr_{0.15}Ca_{0.15}MnO_3$ nanocrystallites on a massive scale, down to tenths of a gram. The nanocrystallites were sintered at different temperature to better understand the impact of temperature on $La_{0.7}Sr_{0.15}Ca_{0.15}MnO_3$ characteristics. XRD and UV-Vis spectroscopes are used to characterise the optical properties of $La_{0.7}Sr_{0.15}Ca_{0.15}MnO_3$ nanocrystallites.

2. Experiment

The $La_{0.7}$ $Sr_{0.15}Ca_{0.15}MnO_3$ nanocrystalline was prepared with their nitrate precursors of La $(NO_3)_3$.6H2O, $Sr(NO_3)_2$, $Ca(NO_3)_2.4H_2O$ and $Mn(NO_3)_2.4H_2O$ of 99.99% purity AR grade compounds. These starting compounds with their stoichiometry were separately dissolved in de-ionised water and mixed in a beaker to form a desired precursor solution. The stoichiometric volume of citric acid ($C_6H_8O_7$) was mixed with precursors solution and placed on a magnetic stirrer for continuous stirring to get a white precipitate solution. The citric acid to nitrate ions molar ratio was set to 1:3. To neutralise, Ammonia (NH_3) was added to this solution drop by drop till pH reaches to 7 and the solution becomes thick brown in colour. The mixture was heated at 60℃ with steady stirring of 400rpm for 3h and stoichiometric volume of ethylene glycol was added. The chelating agent was citric acid solution, whereas the jellification agent was ethylene glycol. This solution was heated continuously at 100℃ until it

changes over into gel. Then the solution was heated to 300℃ until it was totally singed and shaped a free dark powder [22]. The obtained powder was grounded fine and divided into four parts and annealed separately at 700℃,900℃,1100℃, and 1300℃ for 4 hours to get $La_{0.7}Sr_{0.15}Ca_{0.15}MnO_3$ various sized nanocrystallites.

The crystalline structure, crystalline size, and crystal phase identification of $La_{0.7}Sr_{0.15}Ca_{0.15}MnO_3$ nanocrystallites were obtained by X-ray powder diffraction (XRD) method with incident radiation of CuKα (λ=1.5418Å) using Rigaku (Miniflex-II) diffractometer with 0.02degree step size and 2theta angular range from 20° to 80°. Optical properties have been evaluated using UV-Vis spectroscopy (SYSTRONICS DOUBLE BEAM). The optical absorbances were acquired by ultrasonic assisted by dispersing a small quantity of sample in distilled water, data was captured in the 200-800 nm range.

3. Result and Discussion

3.1: XRD Pattern Analysis: The room-temperature XRD pattern of $La_{0.7}Sr_{0.15}Ca_{0.15}MnO_3$ nanocrystallites annealed at 700, 900,1100, 1300℃ were shown in the Figure (1). These XRD patterns confirmed the formation of pure and single phased Rhombohedral structure with space group $R\bar{3}c$ .The intensity of prominent peak for 1300℃ formed at 32.8° was substantially higher than others because of the high crystallinity. The average crystallite size was measured using Debye-Scherrer expression.

$$D = \frac{K\lambda}{\beta\cos\theta} \dots\dots\dots\dots (1)$$

where 'D'is the average crystalline size, K is the shape factor 0.9, and β is the Full width half maximum of peak.

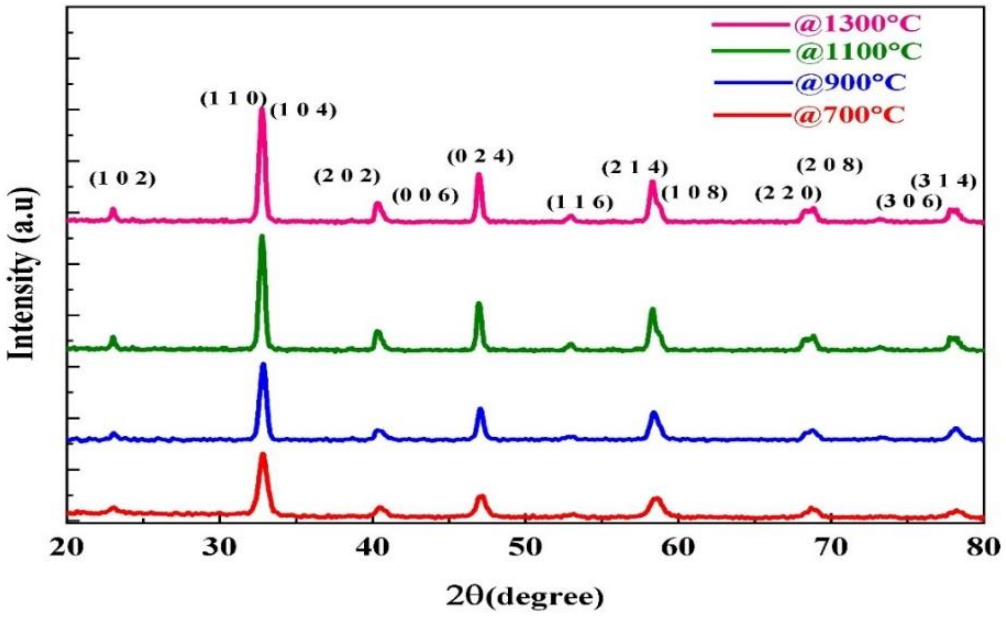

Figure 1: XRD Pattern of the $La_{0.7}Sr_{0.15}Ca_{0.15}MnO_3$ nanocrystallites annealed at 700, 900, 1100, and 1300℃.

It was observed that full width half maximum values were decreased, and average crystallite size values were increased from 15.64 to 36.78 nm with the annealed temperature, which are given in Table 1.

Micro strain values are calculated from the equation [23].

$$\varepsilon = \frac{\beta}{4 \tan \theta} \ldots\ldots\ldots (2)$$

The micro strain values were observed to be in the range from 7.86×10^{-3} to 3.34×10^{-3} as a function of annealed temperature.

Dislocation density values were calculated using the following equation [23].

$$\delta_D = \frac{1}{D^2} \ldots\ldots\ldots\ldots\ldots\ldots\ldots (3)$$

Dislocation density values of were changed from 4.088×10^{-3} nm^{-2} to 0.739×10^{-3} nm^{-2} as the annealed temperature increased from 700℃ to 1300℃.

Table–1: Structural and Optical parameters of $La_{0.7}$ $Sr_{0.15}Ca_{0.15}MnO_3$ nanocrystallites at annealed temperature 700, 900, 1100, and 1300℃.

Annealed Temperature	**700°C**	**900°C**	**1100°C**	**1300°C**
Crystallite Size D (nm)	15.64	19.46	23.18	36.78
Dislocation density (δ_D) (nm^{-2})$\times10^{-3}$	4.088	2.645	1.865	0.739
Micro strain (ε)$\times10^{-3}$	7.86	6.30	5.31	3.34
Absorption peak(nm)	447.2	448.7	448.9	468.8
Band gap (eV)	3.59	3.53	3.45	3.41

3.2: UV-Vis spectroscopic analysis:

The main physical features that describe the optical properties of $La_{0.7}$ $Sr_{0.15}Ca_{0.15}MnO_3$ nanocrystallites are the energy gap and refractive index. Figure 2(a-b) indicates the variation of absorbance and transmittance spectra of the $La_{0.7}$ $Sr_{0.15}Ca_{0.15}MnO_3$ annealed at 700, 900, 1100, and 1300℃. A sharp absorption edge was identified in the range 447 - 468 nm in the visible region for all prepared samples. The expressions (4,5,6) were used to calculate the absorption coefficient of $La_{0.7}$ $Sr_{0.15}Ca_{0.15}MnO_3$ nanocrystallites [24,25].

$$I = I_0 e^{\propto t} \ldots\ldots\ldots (4)$$

$$A = log \frac{I_0}{I} \ldots\ldots\ldots (5)$$

$$\alpha = \frac{2.303\, A}{t} \ldots\ldots\ldots (6)$$

where ‘α’, ‘A’ and ‘t’ are the absorption coefficient, absorbance, and sample thickness respectively.

The transmittance (T_s)was measured applying the relation (7).

$$T_s=10^{-A} \times 100 \ldots\ldots\ldots\ldots (7)$$

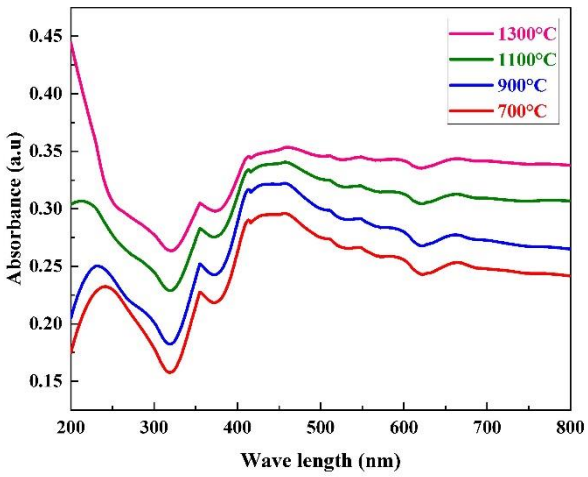

Figure 2(a)

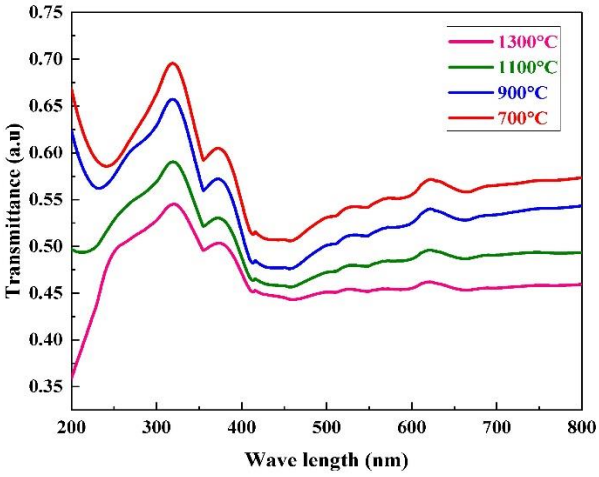

Figure 2(b)

Figure 2(a-b): UV-Vis Absorbance and Transmittance of the $La_{0.7}Sr_{0.15}Ca_{0.15}MnO_3$ annealed at 700,900,1100, and 1300°C.

The refractive index (n) was measured by the below relation.

$$n = \frac{1}{T_s} + \sqrt{\frac{1}{T_s - 1}} \ldots\ldots\ldots\ldots\ldots\ldots\ldots\ldots (8)$$

Figure 3 shows the variation of refractive index of the $La_{0.7}Sr_{0.15}Ca_{0.15}MnO_3$ annealed at 700,900,1100, and 1300°C, it clearly reveals that refractive index value increases rapidly and gets maximum value and then decreases in the UV region and the same variation was observed in the visible region for all the samples.

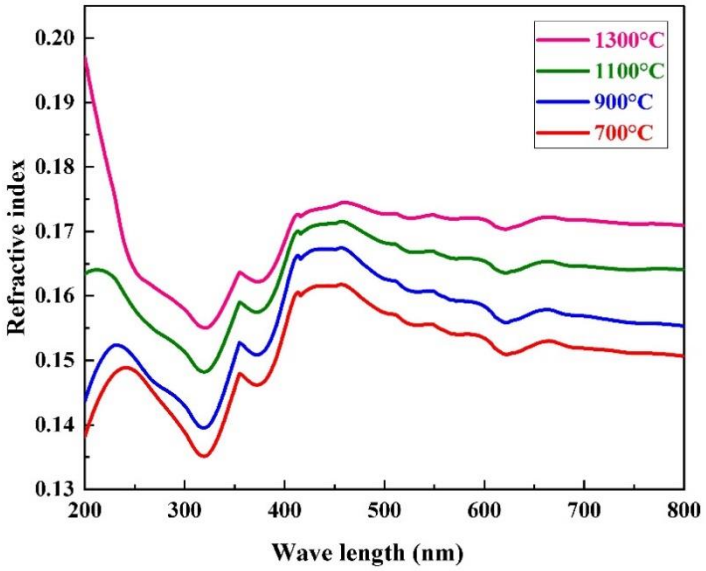

Figure 3: **V**ariation of refractive index of the $La_{0.7}Sr_{0.15}Ca_{0.15}MnO_3$ annealed at 700,900,1100, and 1300°C.

The extinction coefficient(k) was calculated using the relation [26].

$$k = \frac{\alpha\lambda}{4\pi} \ldots\ldots\ldots\ldots\ldots\ldots (9)$$

Figure 4 shows the variation of extinction coefficient of the $La_{0.7}Sr_{0.15}Ca_{0.15}MnO_3$ annealed at 700,900,1100, and 1300℃.It has observed that extinction coefficient increases with the annealed temperature.

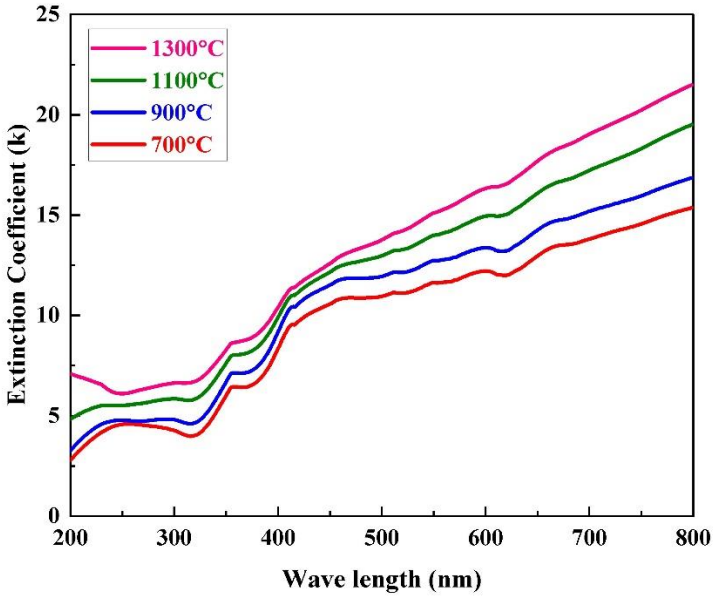

Figure 4: Variation of extinction coefficient of the $La_{0.7}Sr_{0.15}Ca_{0.15}MnO_3$ annealed at 700,900,1100, and 1300℃.

The reflectance of all $La_{0.7}Sr_{0.15}Ca_{0.15}MnO_3$ nanocrystallites was evaluated by the formula [27].

$$R = \frac{(n-1)^2}{(n+1)^2} \ldots\ldots\ldots\ldots\ldots\ldots (10)$$

Figure 5 shows the variation of reflectance of the $La_{0.7}Sr_{0.15}Ca_{0.15}MnO_3$ annealed 700,900,1100, and 1300℃. The reflectance value increases to maximum value then drops in the ultraviolet range and then increases in the visible range.

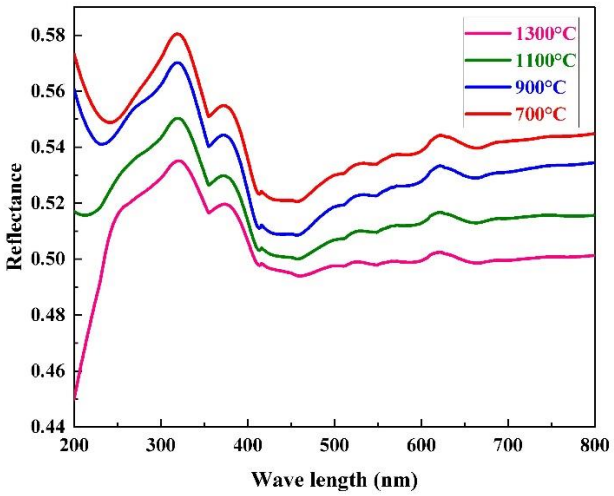

Figure 5: **V**ariation of Reflectance of the $La_{0.7}Sr_{0.15}Ca_{0.15}MnO_3$ annealed at 700,900,1100, and 1300℃.

The real and imaginary part of dielectric constants were evaluated by the expressions [28].

$$\varepsilon_i = 2nk \quad \ldots\ldots\ldots\ldots\ldots\ldots\ldots (11)$$

$$\varepsilon_r = n^2 - k^2 \quad \ldots\ldots\ldots\ldots\ldots\ldots\ldots (12)$$

Figure 6(a & b) gives similarities of the real part (ε_r) and the imaginary part (ε_i) of dielectric constant of the $La_{0.7}Sr_{0.15}Ca_{0.15}MnO_3$ nanocrystallites annealed at 700,900,1100, and 1300℃.

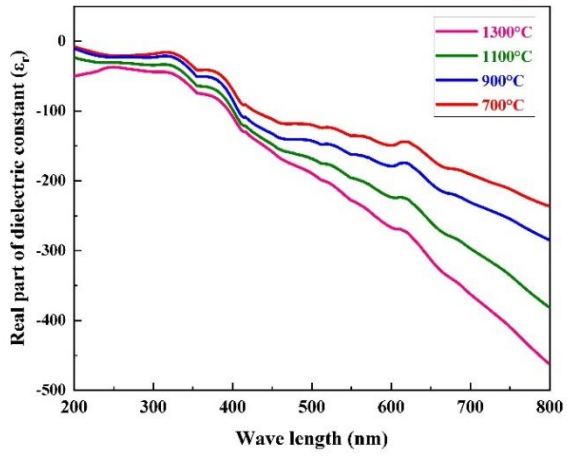

Figure 6(a)

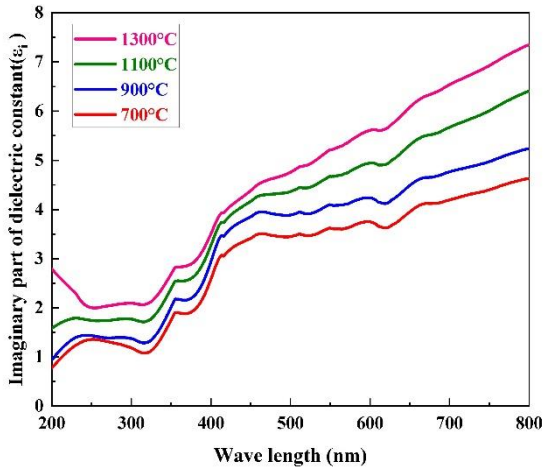

Figure 6(b)

Figure 6 (a-b): **V**ariation of real part and imaginary part of dielectric constant of the $La_{0.7}Sr_{0.15}Ca_{0.15}MnO_3$ annealed at 700,900,1100, and 1300℃.

The Optical band gap of post annealed $La_{0.7}Sr_{0.15}Ca_{0.15}MnO_3$ nanocrystallites were measured using Tauc's relation (13) and obtained by Tauc plots [29].

$$(\alpha h\nu)^n = A\,(h\nu - E_g) \ldots\ldots\ldots\ldots\ldots\ldots (13)$$

where E_g, h, υ, n are the band gap, plank's constant, frequency, and index parameter respectively. 'n' represents nature of electron band transition. There are 4 possible values of 'n' depending upon the nature of the transition which relates n = 1/2 (permissible indirect), n = 1(forbidden indirect), n = 3/2(forbidden direct), and n = 2 (allowed direct) [31]. The Tauc plots of $(\alpha h\nu)^n$ versus photon energy (hν) for different 'n' values for $La_{0.7}Sr_{0.15}Ca_{0.15}MnO_3$ nanocrystallites were plotted. Among all the plots $(\alpha h\nu)^2$ verses (hν) plot has a linear relationship over a wide range as observed, indicates the system take the direct transition in the broad band gap area. Figure 7(a- d) shows Tauc plots of the $La_{0.7}Sr_{0.15}Ca_{0.15}MnO_3$ annealed at 700,900,1100, and 1300°C.

The optical energy bandgap of samples was reported by the extrapolating the proportionality section of the graph on the 'hν' axis. The optical band gap values for $La_{0.7}Sr_{0.15}Ca_{0.15}MnO_3$ post annealed nanocrystallites are provided in Table 1, suggests that optical gap decreases from 3.59 eV to 3.41eV with raise in annealing temperature. So, because of optical energy gap as a function of temperature (red shift) were ascribed to increase in particle size, which was corelated to XRD results. The prepared samples are found to be great choices for photocatalytic activities based on the band gap energy values [30].

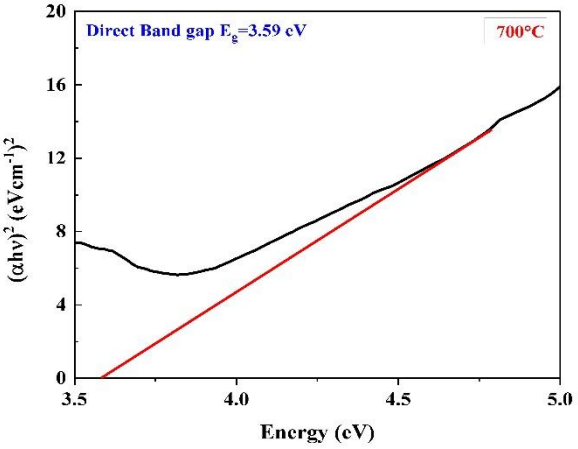

Figure 7 (a)

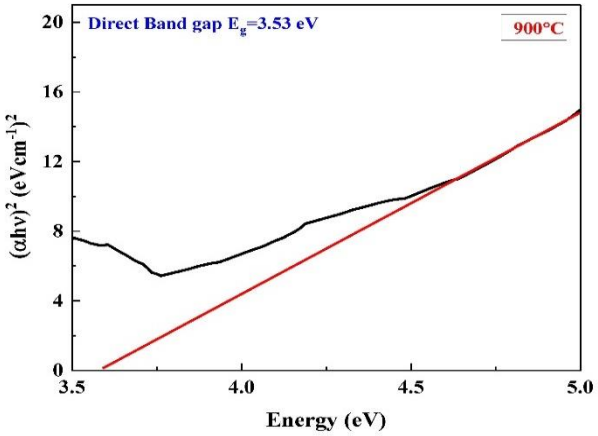

Figure 7 (b)

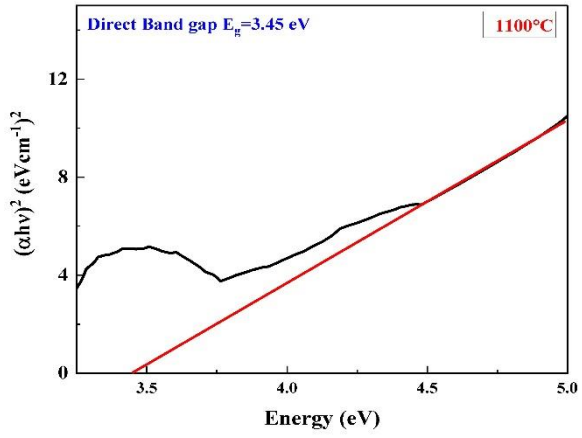

Figure 7 (c)

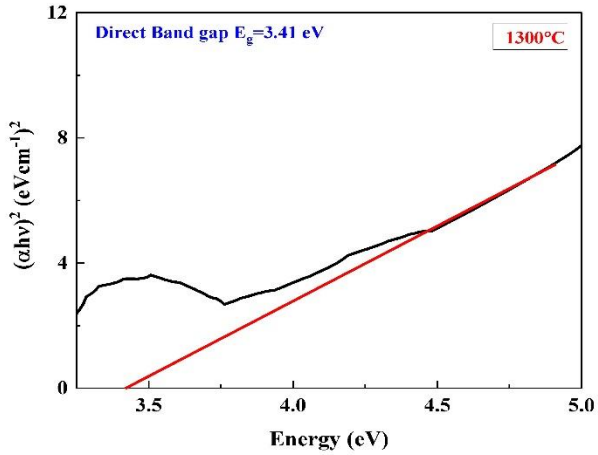

Figure 7 (d)

Figure 7 (a-d): UV-Vis absorbance -Tauc plot of variation of $(\alpha h\nu)^2$ versus photon energy "hν" of the $La_{0.7}Sr_{0.15}Ca_{0.15}MnO_3$ nanocrystallites annealed at 700,900,1100, and 1300°C.

4.Conclusions

1. The $La_{0.7}Sr_{0.15}Ca_{0.15}MnO_3$ nanocrystalline was successfully synthesised using the method of Solgel-combustion method and annealed at 700,900,1100, and 1300°C to get various crystalline sizes.
2. The X ray diffraction confirmed the establishes the rhombohedral structure with space group $R\bar{3}c$ without any impurity peaks. This method of synthesis was produced nanocrystallites with average crystallite size from 15.64 to 36.78nm.
3. For all $La_{0.7}Sr_{0.15}Ca_{0.15}MnO_3$ samples, the dislocation densities were reduced from 4.088×10^{-3} nm^{-2} to 0.739×10^{-3} nm^{-2}, and micro strain values were also decreased from 7.86×10^{-3} to 3.34×10^{-3} as the annealed temperature increases from 700 to 1300°C.
4. The characteristic absorbance peaks were obtained in the range 447.2nm- 468.8nm.
5. UV-vis spectroscopic studies showed that the optical band gap values decreased from 3.59 to 3.41 eV as annealed temperature increased from 700 to 1300°C.

Hence, the optical characteristics of prepared $La_{0.7}Sr_{0.15}Ca_{0.15}MnO_3$ nanocrystallites were influence strongly by the sintering temperature and crystallite size.

References

[1] V. Franco, J.S. Blazqee, J.J. Ipus, J.Y. La, L.M. Moreno, A. Conde, Magnetocaloric effect: from materials research to refrigeration devices, Prog. Mater, Sci.93 (2018) 112-232, https://doi.org/10.1016/j.pmatsci.2017.10.005

[2] V.K. Pecharsky, K.A. Gschneidner Jr., Magnetocaloric effect and magnetic refrigeration, J. Magn. Mag. Mater.200 (1999) 44-56.

[3] T.D. Thanh, L.H. Nguyen, D.H. Manh, N.V. Chien, P.T Phog, N.V. Khiem, L.V. Hong, N.X. Phuc, Structural, magnetic and magneto transport behaviour of La0.7SrxCa0.3-xMnO3 compunds, Physica B: Condensed Matter, 407 (2012) 145-152.

[4] A. Gaur, G.D. Varma, Sintering temperature effect on electrical transport and magnetoresistance of nano phasic La0.7Sr0.3MnO3. J Phys: Condens Matter, 18(2006) 8837- 8846.

[5] S. Zhao, X.-J. Yue, Liu, Influence of Sr doping on structural, electrical, and magnetic properties of La0.7Ca0.3MnO3 nanoparticles, Ceram Int, 43 (2017) 13240-13246.

[6] U. Shankar, A.K Singh, Origin of Suppression of Charge Ordering Transition in Nanocrystalline Ln0.5Ca0.5MnO3 (Ln=La, Nd, Pr) Ceramics, The Journal of Physical Chemistry C,119(2015)28620-28630.

[7] W. Xia, L. Li, H. Wu, P. Xue, X. Zhu, Structural, morphological, and magnetic properties of sol-gel derived La0.7Ca0.3MnO3 manganite nano particles, Ceram Int, 43(2017)3274-3283.

[8] N. Zaidi, S. Mnefgui, A. Dhahri, J. Dhahri, E.K. Hlil, Study of electrical transport and magneto resistive properties of La0.67-x DyxPb0.33MnO3 (X = 0.00,0.01 and 0.15) J. AlloysComp.616(2014)378-384.

[9] H. Nakatsugawa, M. Saito, and Y. Okamoto, "High-temperature thermoelectric properties of perovskite -type Pr0.9Sr0.1Mn1-xMn1-xFexO3 ($0 \le x \le 1$)," Journal of Electronic materials, vol. 46(2017), pp.3262-3272.

[10] Y. Tokura, “Critical feature of colossal magneto resistive manganites” Reports on Progress in Physics, vol.69, (2006) p.797.

[11] C.B. Larsen, S. Samothrakitis, A.D. Fortes, A.O. Ayas, M. Akyol, A. Ekicibil, and M. Laver, “Basal plane ferromagnetism in the rhombohedral manganite La0.85Ag0.15MnO3+δ,” Journal of Magnetism and Magnetic Materials, vol.498, (2020), p.166193.

[12] M.K. Verma, N.D. Sharma, S. Sharma, N. Choudhary, and D. Singh. “High magnetoresistance in La0.5Nd0.15Ca0.25A0.1MnO3 (A = Ca, Li, N, K) CMR manganites: Correlation in La0.5 Nd0.15 Ca0.25A0.1MnO3, “Material Research Bulletin, vol.125(2020) pp.10813.

[13] S. Biswas, and S. Keshri, “Large magnetocaloric effect near temperature in La0.67(Sr, K/Pb)0.33MnO3 manganite nanomaterials, “Journal of Materials Science: Materials in Electronics, vol 31 (2020) pp. 21896-21912.

[14] L. Joshi, S.S. Rajput, and S. Keshri, “Structural and magneto transport properties of LCMO- STO composites.” Phase Transitions, vol 83 (2010) pp. 482.

[15] D.H. Manh, P.T. Phong, T.D. Thanh, D.N.H. Nam, L.V. Hong, N.X. Phuc, Size effects and interaction in La0.7Ca0.3MnO3 nanoparticles, J Alloy Comp, 509(2011) 1373-1377.

[16] K. Navin, R. Kurchania, The effect of particle size on structural, magnetic and transport properties of La0.7Sr0.3MnO3 nanoparticles, Ceram Int, 44 (2018) 4973-4980.

[17] M. Oumezzine, O. Pene, T. Guizourn, R. Lebullenger, M. Oumezzine, Impact of the sintering temperature on the structural, magnetic, and electrical transport properties of doped La0.67Ba0.33Mn0.9Cr0.1O3 manganite, J Magn Magn Mater, 324(2012) 2821-2828.

[18] M. Rosic, L. Kljaljevic, D. Jordanov, M. Stoiljikovic, V. Kusigerski, V. Spasojevic, B. Matovic, Effects of sintering on the structural, micro structural and magnetic properties of nanoparticle manganite Ca1-xGdxMnO3 (x = 0.05, 0.1, 0.15, 0.2), Ceram Int, 41 (2015) 14964-14972.

[19] G. Alejandro, M. Tovar, A. Butera, A. Caneiro, M.T. Causa, F. Prado, R. Sanchez, Magnetism and Jahn-Teller distortion in La MnO3+d. Phys B: Condensed Matter (2000), 284-288(2):1408.

[20] G.C. Rout, N. Behera, S.N. Behera The influence of band Jahn- Teller effect and magnetic order on the magnetoresistance in manganite system, Phys B: (2009),404(16)2315.

[21] M.H. Phan S.C. Yu, N.H. Hur, Excellent magnetocaloric properties of La 0.7 Ca0.3-x Srx MnO3 single ($0.05 \leq x \leq 0.25$), Appl. Phys. Lett, 86(7) (2005) 072504.

[22] W. Xia, K. Leng, Q. Tang, et al. Comparative studies on the structural, magnetic, and optical properties of perovskite Ln0.67 Ca0.33MnO3 (Ln = La, Pr, Nd, and Sm) magnetic nanoparticles synthesized by sol-gel method: AIP Advances 11,035007 (2021).

[23] D.K. Pawar, S.M. Pawar, P.S. Patil, and S.S. Kolekar, Synthesis of Nanocrystalline Nickel-Zinc Ferrite (Ni0.8Zn0.2Fe2O4) Thin Films by Chemical Bath Deposition Method. Journal of Alloys and Compounds, 509,3587-3591.

[24] H.M. Pathan, J.D. Desai, C.D. Lokhande, Modified Chemical Deposition abd Physico-Chemical Properties of Copper Sulphide (Cu2S) Thin Films, Applied Surface Science, 202,47-56.

[25] M. Srivastava, A.K. Ojha, S. Chaubey, A. Materny, Synthesis and Optical Characterization of Nanocrystalline NiFe2O4 Structures. Journal of Alloys and Compounds, (2009),481,515-519.

[26] S.W. Xue, X.T. Zu, W.L. Zhou, H.X. Deng, X. Xiang, L. Zhang, H. Deng, Effects of post-thermal annealing on the optical constants of ZnO thin film.Journal of Alloy and compounds, (2008),448,21-26.

[27] A. Ashour, N. El-Kadry, S.A. Mahmoud, the electrical and optical properties of CdS films thermally deposited by a modified source, Thin solid films (1995), 269,117-120.

[28] E. Guneri, A. Kariper, Optical properties of amorphous Cus thin films deposited chemically at different pH values. Journal of Allys and Compounds, (1995) 516, 20-26.

[29] U. Kumar, D. Yadav, S. Upadhyay, Investigating of structural, optical, and magnetic properties of Nd-doped Sr2SnO4 Ruddlesden popper oxide. J Am Ceram Soc (2020) 103, 5743-5757.

[30] U. Kumar, D. Yadav, A.K. Thakur, K.K. Srivastav, S. Upadhyay, Investigation on phase formation of Sr2SnO4 and effect of La doping on its structural and optical properties. J Therm Anal Calorim (2018), 135, 1987-1999.